



# Neutron-gamma discrimination method based on blind source separation and machine learning

Hanan Arahmane<sup>1,2</sup> · El-Mehdi Hamzaoui<sup>3</sup> · Yann Ben Maissa<sup>4</sup> ·  
Rajaa Cherkaoui El Moursli<sup>2</sup>

Received: 31 August 2020 / Revised: 3 November 2020 / Accepted: 1 December 2020 / Published online: 17 February 2021  
© China Science Publishing & Media Ltd. (Science Press), Shanghai Institute of Applied Physics, the Chinese Academy of Sciences, Chinese Nuclear Society 2021

**Abstract** The discrimination of neutrons from gamma rays in a mixed radiation field is crucial in neutron detection tasks. Several approaches have been proposed to enhance the performance and accuracy of neutron-gamma discrimination. However, their performances are often associated with certain factors, such as experimental requirements and resulting mixed signals. The main purpose of this study is to achieve fast and accurate neutron-gamma discrimination without a priori information on the signal to be analyzed, as well as the experimental setup. Here, a novel method is proposed based on two concepts. The first method exploits the power of nonnegative tensor factorization (NTF) as a blind source separation method to extract the original components from the mixture signals recorded at the output of the stilbene scintillator detector. The second one is based on the principles of support vector machine (SVM) to identify and discriminate these components. In addition to these two main methods, we adopted the Mexican-hat function as a continuous wavelet transform to characterize

the components extracted using the NTF model. The resulting scalograms are processed as colored images, which are segmented into two distinct classes using the Otsu thresholding method to extract the features of interest of the neutrons and gamma-ray components from the background noise. We subsequently used principal component analysis to select the most significant of these features which are used in the training and testing datasets for SVM. Bias-variance analysis is used to optimize the SVM model by finding the optimal level of model complexity with the highest possible generalization performance. In this framework, the obtained results have verified a suitable bias-variance trade-off value. We achieved an operational SVM prediction model for neutron-gamma classification with a high true-positive rate. The accuracy and performance of the SVM based on the NTF was evaluated and validated by comparing it to the charge comparison method via figure of merit. The results indicate that the proposed approach has a superior discrimination quality (figure of merit of 2.20).

This work was supported by L'Oréal-UNESCO for the Women in Science Maghreb Program Grant Agreement No. 4500410340.

✉ Hanan Arahmane  
hanan.arahmane@cea.fr

<sup>1</sup> Université Paris-Saclay, CEA, List, 91120 Palaiseau, France

<sup>2</sup> Equipe des Sciences de la Matière et du Rayonnement (ESMaR), Faculty of Sciences, Mohammed V University in Rabat, B.P. 1014 RP, Rabat, Morocco

<sup>3</sup> National Centre for Nuclear Energy, Science and Technology (CNESTEN), B.P. 1382 R.P. 10001, Rabat, Morocco

<sup>4</sup> Laboratory of Telecommunications, Networks and Service Systems, National Institute of Posts and Telecommunications, Allal El Fassi Avenue, Rabat, Morocco

**Keywords** Blind source separation · Nonnegative tensor factorization (NTF) · Support vector machines (SVM) · Continuous wavelets transform (CWT) · Otsu thresholding method

## 1 Introduction

Although organic scintillator detectors have been commonly used for neutron measurement systems owing to their high efficiency, they are too sensitive to gamma rays. Several methods have been proposed to reduce the effect of gamma rays on the neutron detection results. Pulse shape

discrimination (PSD) [1] is a popular method used for neutron-gamma discrimination. Several digital and analog PSD approaches have been proposed to perform this task, such as the rise time [2], charge comparison (CCM) [3, 4], zero-crossing [5, 6], pulse gradient analysis (PGA) [7], and wavelet transform [8]. However, these methods are limited in discriminating small difference pulses, as well as multiple pulses.

With progress in data acquisition systems, new possibilities in digital pulse processing have opened up for organic scintillator detectors [9]. Currently, machine learning has proven to be a powerful tool in the analysis of radiation data. Its algorithms use simple and direct methods to learn information from a dataset without a predetermined model [10]. According to a priori knowledge in the modeling procedure, machine learning methods can be divided into two classes: supervised machine learning using a priori knowledge and unsupervised machine learning without prior knowledge.

In most neutron spectroscopy applications, PSD is used to separate neutrons from gamma rays based on the time and energy features of the digitized pulses. However, their effectiveness is associated with a number of elements (*i.e.*, prior information) that can be divided into two categories. First, the experimental setup, which includes the type of scintillator detector used, experimental needs, and data acquisition system. Second, the processing phase, which represents the signal-to-noise ratio (SNR), and the difference between the pulses, as well as pile-up. The main challenge in these studies involves the means to realizing fast and accurate neutron-gamma discrimination without any a priori information on the signal to be analyzed (*i.e.*, processing phase), as well as the experimental setup.

To overcome the ineffectiveness of PSD's performance, other methods that combine PSD with machine learning algorithms, namely, support vector machines (SVMs), have been proposed [11–15]. Nevertheless, the SVM application does not follow certain paramount criteria such as data balance, cross-validation process, and bias-variance analysis, which provide more accuracy and credibility for neutron-gamma discrimination.

In this study, a novel method was proposed on the basis of machine learning to obtain fast and accurate neutron-gamma discrimination without any a priori information on the signal to be analyzed, as well as the experimental setup. First, we adopted the nonnegative tensor factorization (NTF) model as a blind source separation (BSS) technique to extract the original components from the mixture recorded at the output of a stilbene scintillator detector (45 mm × 45 mm). Second, an SVM was used to identify and discriminate these components. However, before that, Mexican-hat-function-based continuous wavelet transform (CWT) was utilized as a spectral analysis to characterize

these extracted components within the time–frequency domain. The resulting scalograms are viewed as images, which are segmented into two distinct classes using the Otsu thresholding method to extract the features of interest of neutrons and gamma-ray components from the background. We subsequently used principal component analysis (PCA) to select the most significant of these features to form the training and testing datasets for SVM classification purposes. We employed bias-variance analysis to optimize the SVM model by finding the optimal level of model complexity with the highest possible generalization performance. The achieved results have proven a suitable bias–variance trade-off value in this regard. We actually achieved an operational SVM prediction model for neutron-gamma classification with a high true-positive rate. The performance of our proposed method was evaluated and validated by comparing it to the CCM via the figure of merit (FOM). With an FOM value of 2.20, the comparison verified the superiority of the SVM-based over NTF in terms of discrimination quality.

An overview of the present paper is presented here. First, we discuss selected works on this framework in Sect. 2. Then, we focus on describing the analyzed signals, principle of the proposed method, and CCM method used for comparative validation in Sect. 3. Next, we comprehensively discuss the results of the proposed method in Sect. 4 before concluding the paper.

## 2 Related works

Only a few limited works have adopted PSD and SVM in addressing the neutron-gamma discrimination challenge, online or offline [11–14]. The results achieved by these research works are satisfactory, with each one introducing a specific approach to improving neutron-gamma discrimination. However, their effectiveness is associated with various factors, including the PSD requirement of a priori information on the signal to be analyzed, choice of scintillator detector, and acquisition system. Besides these factors, SVM application does not respect some key points such as bias-variance analysis [8–11] and cross-validation process [10–14]. In this section, we present and discuss a selection of these and other works.

Sanderson et al. (2012) [11] applied SVM to determine a PSD classifier. The authors demonstrated that the SVM method coupled with CCM enhances detection performance and provides more precise estimates by considering the necessity of contaminating the training data needed for the SVM. However, the SVM solution proposed by the authors does not meet the basic criteria for its application, such as the cross-validation procedure, computation of generalization performance, and bias-variance analysis.

Yu et al. (2015) [12] proposed the SVM method in conjunction with the moment analysis method (MAM) to achieve neutron-gamma discrimination of pulses from an organic liquid scintillator. They used the CCM method to discriminate neutrons and gamma-ray pulses, which form the training and testing datasets for the SVM. Then, MAM was applied to create the feature vectors for each pulse in the datasets. The authors demonstrated that the SVM classifier coupled with MAM has exhibited a great ability to separate the neutrons and gamma-ray pulses while providing the classification accuracy for each pulse type. However, its performance is limited because of the neglected data balance in the prediction phase, as well as the evaluation of the SVM model complexity using bias-variance analysis.

Zhang et al. (2018) [13] presented a method based on the SVM discriminator for discriminating neutrons from gamma-ray backgrounds and enhancing the performance of the time-of-flight neutron detector (EJ-299-33 plastic scintillator with PSD property). The proposed method has been implemented in field-programmable gate arrays (FPGAs) to detect neutrons in mixed radiation fields. The obtained results show that real-time neutron-gamma discrimination was achieved with a discrimination accuracy of 99.1%, which could be better with bias-variance analysis.

Zhang et al. (2019) [14] presented a direct method to discriminate nuclear pulse shapes based on PCA and SVM. The authors determined that the training and testing accuracies of SVM classifiers are all above 94.7% provided appropriate kernels are well selected. However, the performance accuracy was less than that obtained by Zhang et al. (2018) and Yu et al. (2015). Furthermore, the selection of the Gaussian kernel most adapted to their study was not based on the grid search and stratified  $K$ -fold cross-validation used to set its hyperparameters.

In our previous work [16], we introduced a novel method that combines nonnegative matrix factorization (NMF) with SVM to perform neutron-gamma discrimination at the output of a stilbene detector. We used the Otsu thresholding method based on CWT to extract the main features of neutrons and gamma-ray signals that have been extracted by the NMF method. These features were then fed into a nonlinear SVM classifier to perform neutron-gamma discrimination. To achieve this, a Gaussian kernel function was selected using grid search and stratified  $K$ -fold cross-validation. The proposed method obtained a good SVM prediction model with a suitable classification rate of 99.93%.

Via the analysis of the works mentioned in this section, we can consider that of Arahmane et al., who presented an approach that does not require any a priori information on the signal to be analyzed, as well as on the experimental setup. In addition, it obeys the true working process of

SVM with an operational prediction model that has provided a better true neutron-gamma classification rate of 99.93%.

To achieve more efficiency and accuracy of this neutron-gamma discrimination process, we have altered the first block of our neutron signal processing chain, as described in [16], which was formed by the second-order NMF separation method. Therefore, in this study, a non-negative parallel factor analysis model (PARAFAC), denoted by the NTF-2 model, is used to achieve a 3D nonnegative tensor factorization of the signals recorded at the output of the stilbene detector. The aim of using the NTF-2 method is based mainly on the fact that it considers both the space and time correlations between the variables more precisely [17], which is very important from the perspective of data processing to optimize the performance of the SVM model.

### 3 Materials and methods

In this section, we present the dataset used for the evaluation of the proposed method, and then the principle of this method, as well as the CCM method, which is used later for comparative verification.

#### 3.1 Dataset characteristics

In this study, the datasets are composed of 100 neutrons and gamma-ray signals of 1000 samples each. Figure 1 illustrates an example of 2 consecutive stilbene scintillator output signals. The pulses were obtained based on the following experimental setup: Cf-252 as a mixed neutron-gamma-emitting source and Na-22 as the gamma only source measured through a stilbene crystal scintillator with dimensions of 45 mm  $\times$  45 mm, a RCA7265 photomultiplier tube (PMT) [18], and data acquisition system. It

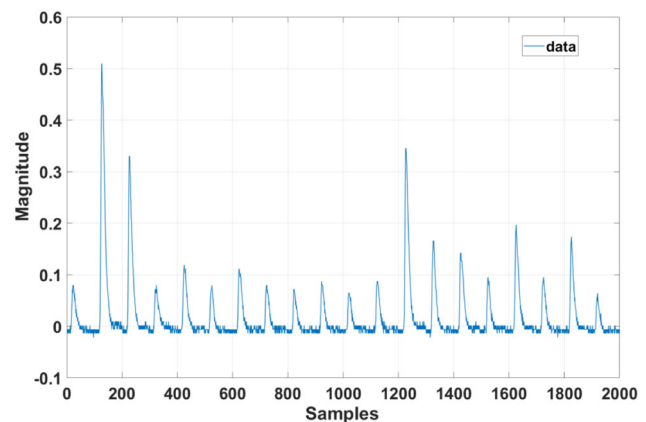


**Fig. 1** Example of two consecutive stilbene scintillator output signals

should be noted that the aim of using Na-22 is to form pure gamma-ray signal set used in the CWT processing step as a reference to confirm the characterization task. The PMT output is connected directly to the ACQIRIS DP210-U1068A using single-ended impedance matching. The ACQIRIS DP210-U1068A is the acquisition system used to digitize the output pulses with 8-bits resolution at a sampling rate of 1 GSamples/s. It is worth noting that the digitizer signal quality is measured by the signal-to-quantization noise ratio (SQNR), which accurately estimates the quality of a b-bit digitizer output [19] as expressed below:

$$SQNR = 1.76 + 6.02b. \tag{1}$$

This corresponds to the fact that the SQNR increases by approximately 6 dB for every bit added to the digitizer word length [19]. Therefore, the sampling rate chosen in our case implies that the analyzed signals have low amplitude. This choice allows us to prove the performance ability of our proposed method in this constraint.

The collected data were stored in a 64-bit computer with 16 Go of RAM for offline processing according to the processing method illustrated in Fig. 1.

### 3.2 Our NTF/SVM method for neutron/gamma discrimination

#### 3.2.1 Method overview

Figure 2 illustrates the steps of our proposed method. We focus on the description of the NTF-2 model. Before that, we provide a brief overview of the other tools used because they are widely described in the literature.

- The CWT is a technique used to carry out signal analysis when the signal frequency varies over time [20, 21]. It is adopted to cut-up the signal using a set of wavelet functions by shifting (time) and scaling (frequency) to a mother wavelet. In our approach, we adopted the Mexican-hat function of the CWT [20] as the mother wavelet because the signal shape is similar to a Gaussian distribution with a long tail on one side [16].

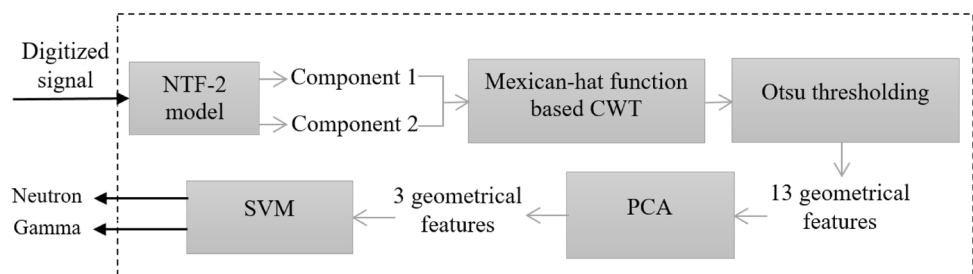
- The Otsu thresholding method enables the determination of an optimal threshold value by minimizing the within-class variance [22]. The selection of the optimal threshold is based on the prior calculation of the gray-level histogram of an image.
- PCA is used in image and signal processing for dimensionality reduction and feature selection [23]. Its main goal is to determine a few linear combinations of the principal components, in which their directions are orthogonal to explain the variance in the data [24].
- SVM was adopted to solve a two-classification problem by determining optimal separation hyperplanes as linear or nonlinear classifiers with maximum margin in a multi-dimensional space [25, 26]. The transformation of the data from the input space into a high-dimensional space requires kernels [27]. The generalization performance evaluation of the SVM model is performed via bias-variance analysis. Determining an optimal bias-variance trade-off helps to achieve good results on unseen datasets [28], thus avoiding deceptive results owing to the inability of the classifier to perform learning generalization (*i.e.*, overfitting phenomenon) [29].

#### 3.2.2 NTF model

NTF (or nonnegative PARAFAC) is a model with nonnegative factor matrices. It is a blind source separation (BSS) method composed of an unsupervised machine learning class used for feature extraction and dimensionality reduction [24]. It should be noted that the BSS method [30, 31] is adopted in signal processing to recover a source signal from a mixture of signals recorded by a sensor without any information about the source signals and/or the mixing procedure. The outputs of digital systems are mostly multi-dimensional and discontinuous. They typically represent one or more variables at a discontinuous set of positions in time and space, and thus are perfect for NTF analysis [32].

We can define the standard NTF model as follows [24, 33, 34]: A given data tensor  $Y \in \mathbb{R}_+^{I \times T \times K}$  is decomposed into a set of matrices  $A \in \mathbb{R}_+^{I \times J}$  and  $X \in \mathbb{R}_+^{J \times T}$  as a

**Fig. 2** Flowchart of proposed neutron-gamma discrimination process



mixing matrix and matrix representing sources (or hidden components), respectively, which can be represented in a slice factorization form [24] as:

$$Y_k = AD_kX + E_k, (k = 1, 2, \dots, K), \tag{2}$$

where  $Y_k = \underline{Y}_{:, :, k} \in \mathbb{R}_+^{I \times T}$  are the frontal slices of a 3D tensor  $\underline{Y} \in \mathbb{R}_+^{I \times T \times K}$ , whereas  $K, D_k \in \mathbb{R}_+^{J \times J}$ , and  $E_k = \underline{E}_{:, :, k} \in \mathbb{R}^{I \times T}$  represent a frontal slice number, diagonal matrix, and  $k$ -th frontal slice of the tensor  $\underline{E}$ , which represents error or noise depending on the application.

To calculate the nonnegative matrices  $\{A, B, C\}$ , we search to minimize (relative to the component matrices) an appropriate cost function by applying the constrained optimization approach [24]. We can express the cost function with nonnegativity constraints as follows [24]:

$$D_F(\underline{Y} || \{A, B, C\}) = \|\underline{Y} - \{A, B, C\}\|_F^2 + \alpha_A \|A\|_F^2 + \alpha_B \|B\|_F^2 + \alpha_C \|C\|_F^2, \tag{3}$$

where  $\alpha_A, \alpha_B, \alpha_C$  are parameters of nonnegative regularization.

The alternating least squares (ALS) method is the most common approach for solving this optimization problem [24] and thus solving the NTF problem. In this approach, we compute the cost function gradient relative to each individual matrix, assuming that the others are independent and fixed [24].

3D NTF-1 and/or 3D NTF-2 [24, 35, 36] models are extensions of the standard NTF (or PARAFAC). In the case of the NTF-1 model, a given tensor  $\underline{Y} \in \mathbb{R}_+^{I \times T \times K}$  is factorized to a set of matrices  $AD$  and  $\{X_1, X_2, \dots, X_K\}$  with nonnegative matrices [24]:

$$Y_k = AD_kX_k + E_k, (k = 1, 2, \dots, K), \tag{4}$$

where  $A \in \mathbb{R}_+^{I \times J}, D_k \in \mathbb{R}_+^{J \times J}, X_k \in \mathbb{R}_+^{J \times T}$ , and  $E_k = \underline{E}_{:, :, k} \in \mathbb{R}^{I \times T}$  represent a mixing matrix, diagonal matrix, matrix of the sources, and  $k$ -th frontal slice of the tensor  $\underline{E} \in \mathbb{R}_+^{I \times T \times K}$  corresponding to the errors or noise.

For the NTF-2 model (similar to the PARAFAC2 model [24, 36]), which is considered as a double model to NTF-1, given by [36]:

$$Y_k = A_k D_k X + E_k, (k = 1, 2, \dots, K), \tag{5}$$

where  $A_k \in \mathbb{R}_+^{I \times J}$  are the mixing matrices,  $D_k \in \mathbb{R}_+^{J \times J}$  is a diagonal matrix,  $X \in \mathbb{R}_+^{J \times T}$  is a matrix representing hidden sources, and  $E_k$  corresponds to error or noise according to the application.

To extract original sources from the recorded mixed signals in this research work, we selected an NTF-2 model

as a more suitable model owing to the form of the column observation vectors.

### 3.3 Alternative method for comparative validation: CCM

CCM [9, 11] is a signal processing technique and a well-known PSD method used for the recognition of gamma-ray and neutron pulses within a mixed radiation field. This method is based on the difference between the expected time distribution for the neutrons with a long tail, including that of the gamma rays with a much shorter tail. It consists of integrating the pulse  $P(t)$  over two distinct time periods,  $Q_{total} = \int_{T_{start}}^T P(t) dt$  as the total integral and  $Q_{tail} = \int_{T_{fast}}^{T_{slow}} P(t) dt$  as a tail integral for the integration of the whole and the tail pulse, as illustrated in Fig. 3. The ratio of the tail-to-total integrals is used to distinguish the pulse origin, mathematically formulated as

$$Ratio = \frac{Q_{tail}}{Q_{total}}. \tag{6}$$

### 3.4 Comparative validation metric

To assess the discrimination ability of the method, we used the figure of merit (FOM) [8, 9, 13] as a discrimination quality metric, formulated as:

$$FOM = \frac{S_{N_\gamma}}{FWHM_N + FWHM_\gamma}, \tag{7}$$

where  $S_{N_\gamma}$  is the separation between the gamma-ray and neutron peaks, and  $FWHM_N$  and  $FWHM_\gamma$  represent their full widths at half maximum (FWHM). We used the Gaussian function to fit the distribution of the neutron and gamma-ray events. A higher FOM value indicates greater quality discrimination.

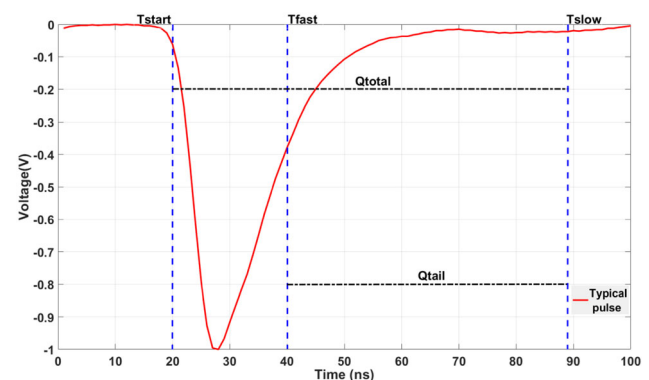


Fig. 3 Example of pulse processing using CCM/PSD method

### 4 Results and discussion

In this section, we present the results of the proposed method mainly based on the SVM and NTF machine learning methods to perform fast and accurate neutron-gamma discrimination. The obtained results for each step of our proposed method are as follows:

#### 4.1 Step1: NTF processing

We consider a set of 10 mixed signals recorded at the output of a stilbene detector sampled at 1 GSample/sec as observations (or a set measured sensor signals) [16, 33]. According to the literature and our previous work [33, 37], the ideal number of signals to be analyzed by a BSS algorithm, which allows an excellent reconstruction of the original sources, is five observations. To apply the NTF-2 model, we form 3D tensors of overlapped sources. For that, the ten mixed signals are structured in six matrices of  $5 \times 1000$  mixtures ( $5 \times 1000$ ) representing observations for which the five nonnegative sources are collected in one slice  $X \in \mathbb{R}_+^{5 \times 1000}$ . We use a common random matrix with a uniform distribution  $A_k \in \mathbb{R}_+^{10 \times 5}$  to mix the sources. Consequently, the 3D tensor of overlapped sources is formed as  $Y \in \mathbb{R}_+^{10 \times 1000 \times 5}$ .

The NTF-2 model applied to these overlapped sources provides a solution to our BSS problem. To validate and determine the accuracy of the separation quality, we compute the signal-to-interference ratio (SIR) to estimate the original sources that comprise the detector mixed output signals. Figure 4 illustrates that the recorded mixed signals are formed by two independent components (ICs:

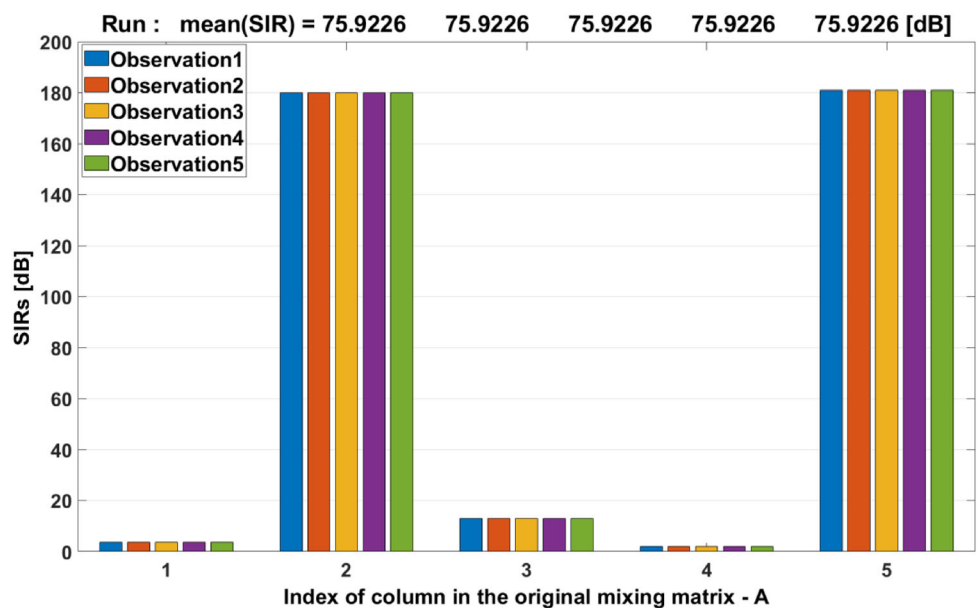
2nd and 5th). We performed the separation task with a mean SIR value of approximately 76 dB, which reflects a very good signal processing performance, as shown in Fig. 4. In fact,  $SIR \geq 30$  dB indicates an optimal separation performance and perfect reconstruction of the original sources [33, 38]. This can also be justified by the fact that the nonnegative tensor factorization methods adopt more projection axes than 2-D to achieve the blind separation task. This allows information to be extracted from different projections (tensors) and therefore results in coherent components that are more independent of each other.

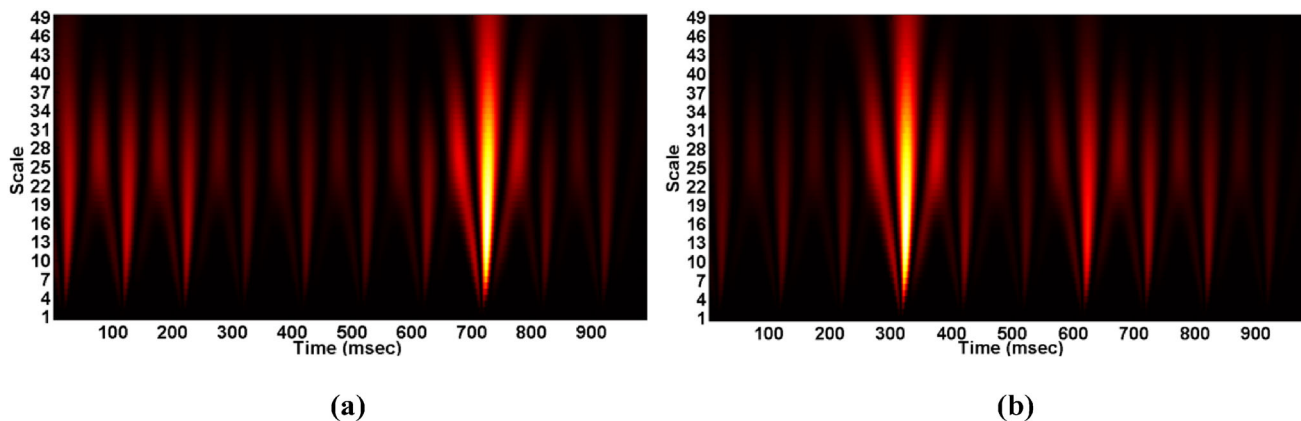
#### 4.2 Step 2: Mexican-hat function-based CWT processing

The characterization of both ICs (IC<sub>2</sub> and IC<sub>5</sub>) was carried out using a Mexican-hat-function-based CWT. We determined that IC<sub>2</sub> and IC<sub>5</sub> have one high-energy zone situated in the same scale range of 5–38 and at different time ranges of 700–720 ms and 300–320 ms, respectively (see Fig. 5). The comparison of both obtained scalograms with those of pure neutrons and gamma-ray signals demonstrates that IC<sub>2</sub> and IC<sub>5</sub> represent the neutrons and gamma-ray signals, respectively.

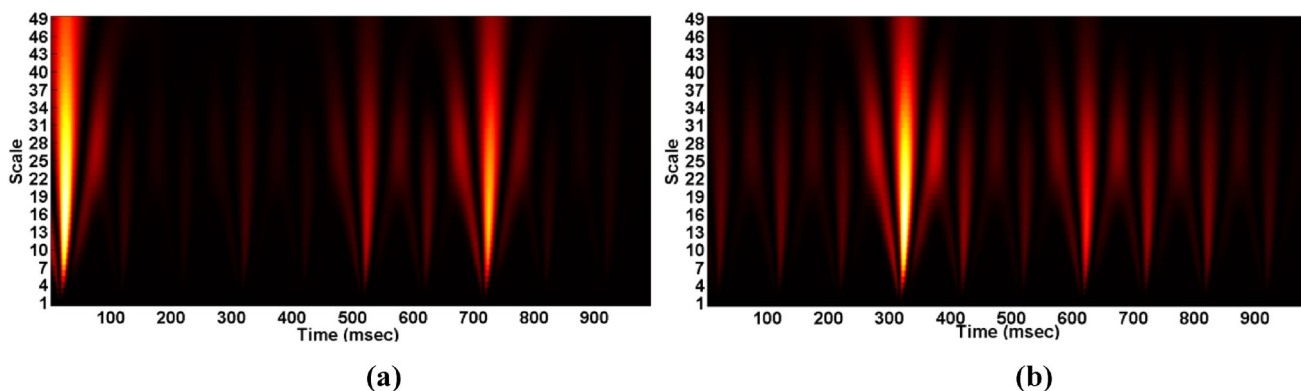
The results of the NMF application [16] have shown that the scalograms of the neutron signal are formed by two main high-energy bands situated at ranges of approximately 0–25 ms and 700–720 ms. These energies appear in the scale range of 7–43 (Fig. 6a). The gamma-ray signal scalograms have only one high-energy band situated at a range of approximately 300–320 ms and scales of 6–35 scales (Fig. 6b). These differences appear owing to the high level of accuracy that the NTF-2 provides while

Fig. 4 (Color online) Plot of SIR as a function of column index in the original mixing matrix-A





**Fig. 5** (Color online) Scalograms of neutron (IC<sub>2</sub>) (a) and gamma-ray (IC<sub>5</sub>) (b) signals resulting from the application of Mexican-hat-function-based CWT for the NTF-2 application



**Fig. 6** (Color online) Scalograms of neutron (a) and gamma-ray (b) signals resulting from the application of Mexican-hat-function-based CWT for the NMF application

extracting the independent components that form the recorded signals. Therefore, the true energy of the signal appears only on its corresponding scalogram.

**4.3 Step 3: otsu thresholding processing**

We conclude that  $T_{\text{Neutron}} = T_{\text{Gamma}} = 0.5098$  (Fig. 7a, b) is the optimal threshold that can be used to segment the neutrons and gamma-ray images (Fig. 7c, d). From each image, we have extracted 13 geometrical features that represent: “ConvexArea”, “Area”, “Eccentricity”, “EquivDiameter”, “MajorAxisLength”, “FilledArea”, “MinorAxisLength”, “Extent”, “PerimeterOld”, “Orientation”, “Solidity”, “EulerNumber”, and “Perimeter” [16].

**4.4 Step 4: principle components analysis processing**

To enhance the prediction ability of the SVM model, we adopted principle component analysis (PCA) to select

significant features among the 13 extracted features. We inferred that “Area”, “MajorAxisLength”, and “MinorAxisLength” are the most useful features (Fig. 8).

**4.5 Step 5: SVM processing**

We use the three selected features as a vector of attributes that are implanted in the SVM model for training, cross-validation, and testing the SVM model.

For the training and cross-validation SVM model, both neutron and gamma-ray datasets were balanced using 2000 binary images (or segmented images) with 1000 images for neutrons labeled  $-1$  and 1000 images for gamma rays labeled  $+1$ . To define the shape of the separation margin used to classify the support vectors, we conducted tests with three kernel functions: linear, polynomial, and Gaussian. The selection of a suitable kernel was based on its configuration that allows for a small generalization error using a cross-validation process. This configuration represents the variation in the SVM model complexity. According to the simulation tests carried out, we

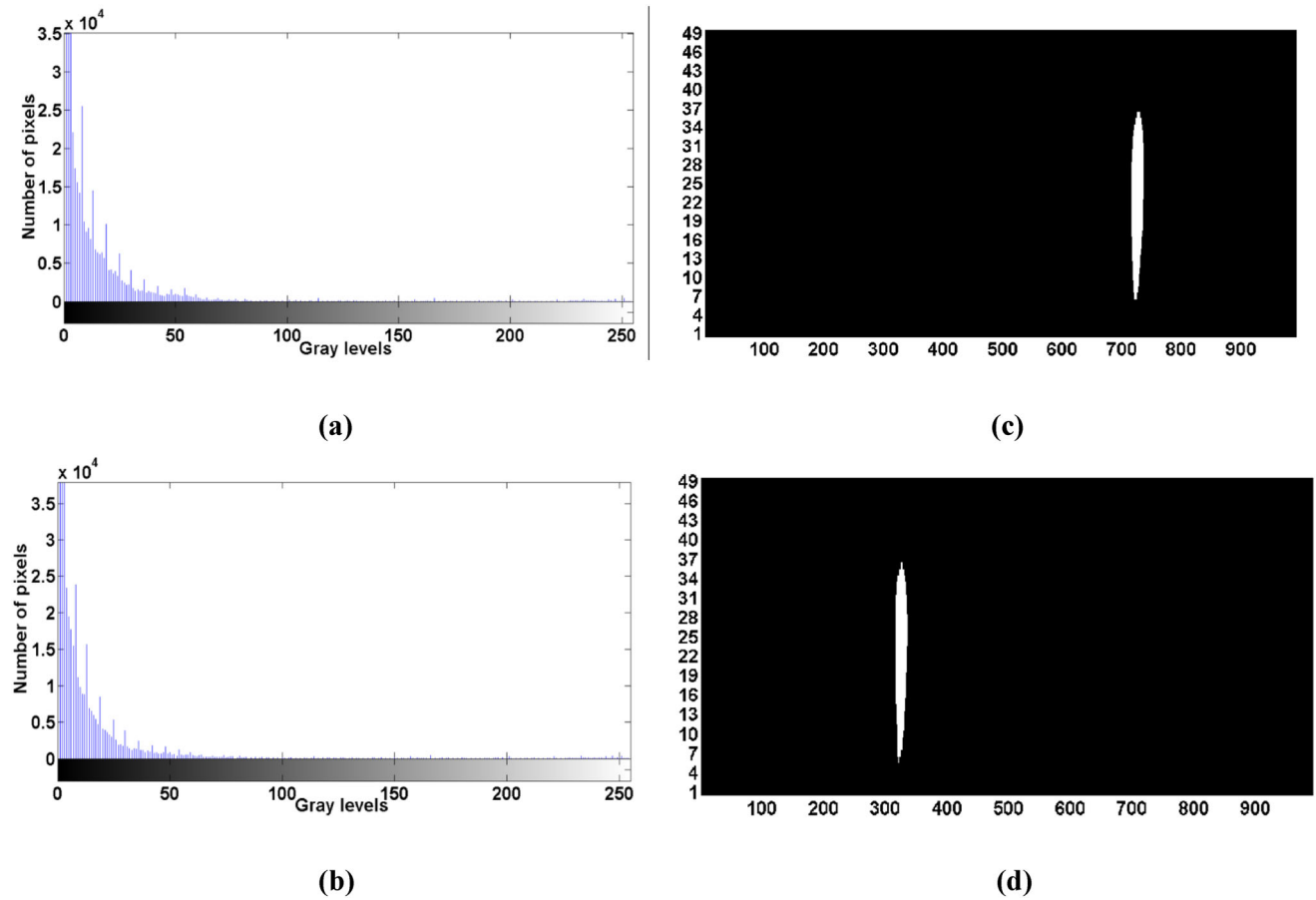


Fig. 7 (Color online) Gray-level histograms of neutron (a) and gamma-ray (b) signals. Binary images of neutron (c) and gamma-ray (d) signals

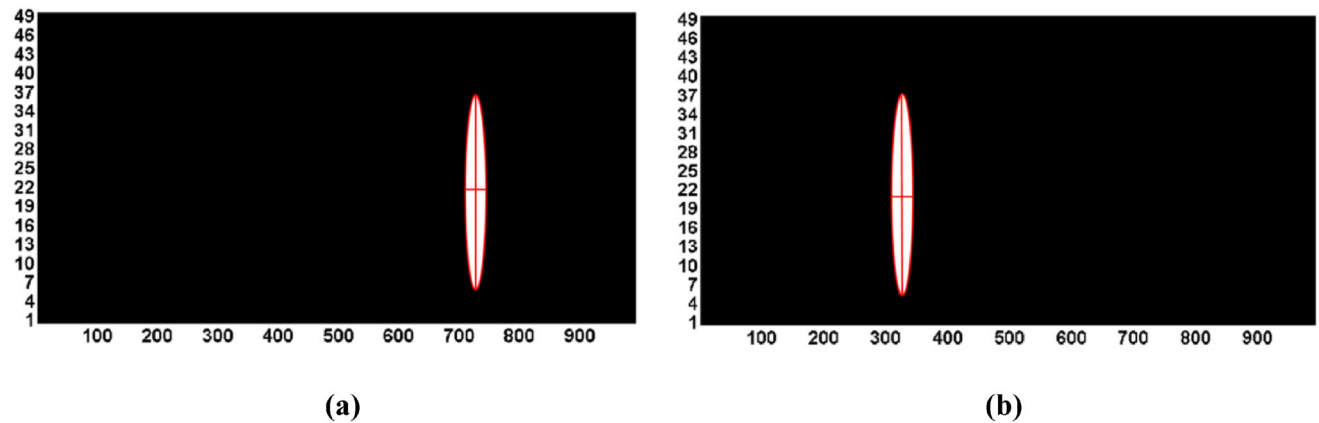
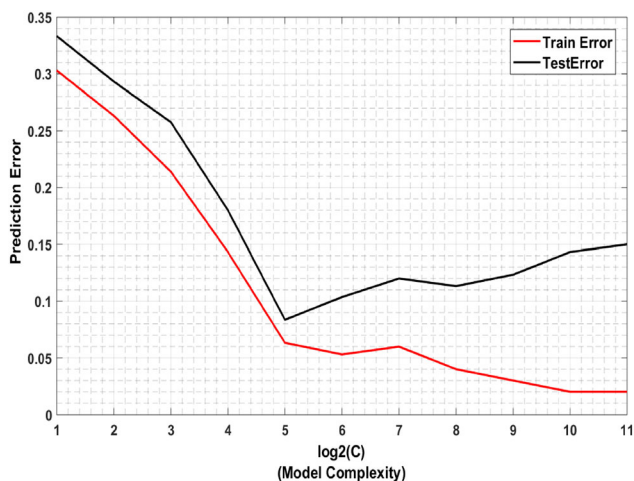


Fig. 8 (Color online) Feature selection of neutron (a) and gamma-ray (b) signals in the binary image, using PCA method

determined that the Gaussian kernel is suitable as it provides a small generalization error (0.04%). Note that the Gaussian complexity is based on two parameters: the penalty coefficient  $C$  and bandwidth  $\gamma$ , which are defined using grid search and stratified  $K$ -fold cross-validations, respectively. To achieve these, we randomly divided the dataset into  $K = 10$  subsets that were used to calculate the

cross-validation with this grid search  $\{C = 2^{-5}, 2^{-3}, \dots, 2^{15}, \gamma = 2^{-15}, 2^{-13}, \dots, 2^3\}$  and finally achieve the best pair  $C = 40$  and  $\gamma = 0.7$ . Figure 9 shows the variation of the prediction error of the train and test dataset as a function of  $\log_2(C)$  model complexity.

From the perspective of bias-variance analysis, a good bias-variance trade-off value between train and test errors



**Fig. 9** (Color online) Evaluation of SVM model using bias-variance analysis based on the cross-validation process

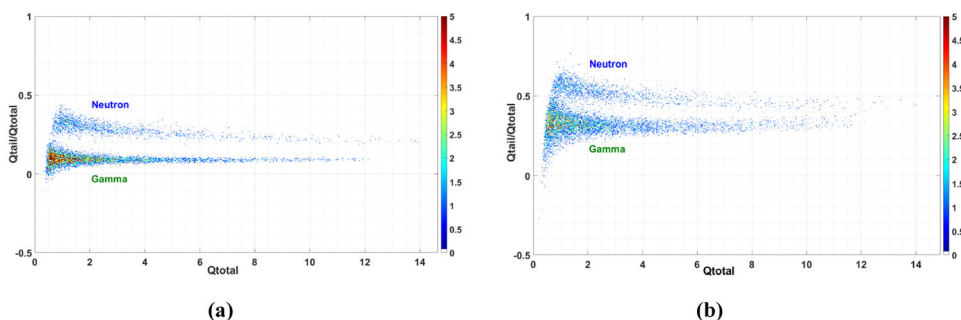
was determined as  $\log_2(C) = 5$ , which demonstrated the capability of our SVM model for maximizing its generalization performance and thus minimizing the prediction error.

To examine the performance of our SVM model, we tested 1000 new images (i.e., 500 images for neutrons and 500 images for gamma rays). We successfully classified 99 images with a high classification rate (99.96%), which completes the efficiency proof of the neutron-gamma discrimination process introduced. Compared to the results obtained in [16], the NMF-SVM method allowed the use of the same kernel function (Gaussian) as a neutron-gamma discrimination with a rate of 99.93%. This rate was achieved using  $C = 32$  and  $\gamma = 0.5$  as the best parameters of the Gaussian function and with a generalization error of 0.065%.

#### 4.6 Performance evaluation

To evaluate and validate the performance of the proposed method, we compared it to CCM/PSD. Figure 10 shows the bi-parametric histogram of the tail-to-total integral as a function of the total integral obtained from a stilbene crystal scintillator and PMT. We can see that the

**Fig. 10** (Color online) Bi-parametric histogram of tail-to-total integral as a function of the total integral obtained from a stilbene crystal scintillator and PMT via SVM based on NTF (a) and CCM/PSD (b)



neutron and gamma-ray regions can be identified visually. As illustrated, there are two classes: the upper class represents neutron pulses and the lower class corresponds to gamma-ray pulses. Therefore, this representation allows the qualitative assessment of the effectiveness of neutron-gamma discrimination methods.

To quantify the obtained results by using NTF/SVM compared to the CCM, the FOM was used (Fig. 11). The computation of the FOM value is determined from the analysis of the tail-to-total integral histogram, which shows that NTF/SVM has a higher FOM (2.20) when compared to the CCM (FOM = 0.99). This clearly indicates the charge distribution of the neutron and gamma-ray events. Consequently, this distribution confirms the results achieved in Fig. 10, thus validating the previous results.

As stated above and based on the achieved results, using the NTF model in the separation task is more efficient than using the NMF algorithm, [13] and it is evident through the higher classification rate obtained (99.96%). From the separation perspective, the NTF model (or PRAFAC model) adopts 3D projection matrices, and thus the separation task is more accurate than the NMF that uses 2D projection matrices. Despite this difference, the obtained results with NMF and/or NTF algorithms of the BSS methods, coupled with SVM, prove its ability to perform accurate neutron-gamma discrimination with a true classification rate as high as that of conventional methods such as a common PSD standard technique. The comparison results show that the FOM provided by the SVM-based NTF method is superior.

### 5 Conclusion

In this study, we proposed a novel method for neutron-gamma discrimination without any a priori information on the signal to be analyzed using NTF/BSS (unsupervised learning method) and SVM (supervised learning method). The first method aims to extract the original components from the mixture signals recorded at the output of the stilbene scintillator detector, while the second method aims

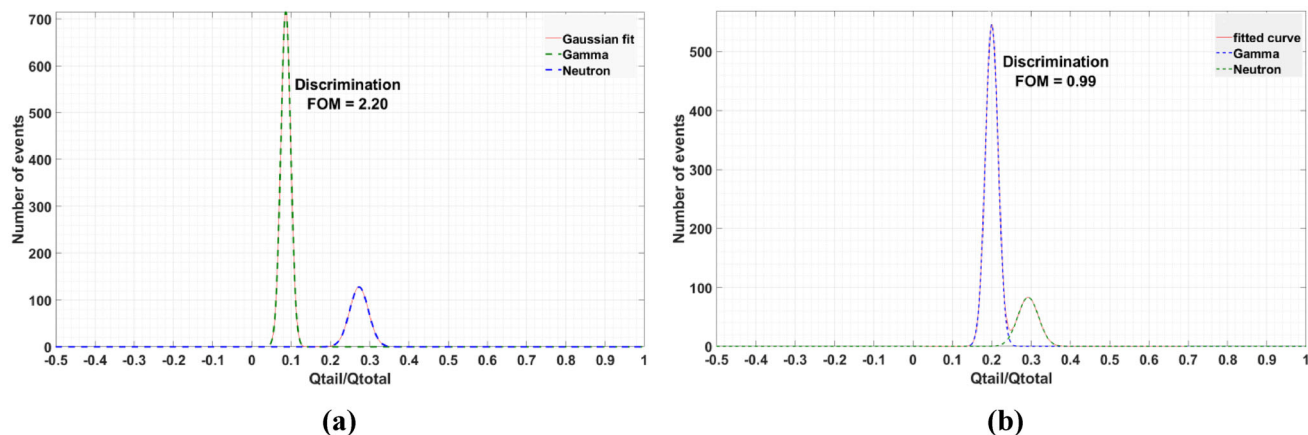


**Fig. 11** (Color online) Histogram analysis of tail-to-total integral obtained from a stilbene crystal scintillator and PMT via SVM based on NTF (a) and CCM/PSD (b)

to classify these components. In addition to SVM, we applied the Mexican-hat-function-based CWT, Otsu thresholding, and PCA methods to improve the prediction ability of our SVM model. Furthermore, we used bias-variance analysis to evaluate the SVM model complexity as it provided an optimal level with the highest possible generalization performance. Furthermore, we compared our method with CCM/PSD for validation. The FOM values obtained using the SVM-based NTF method were determined to be significantly higher ( $FOM = 2.20$ ) than those obtained using CCM. Therefore, all obtained results clearly indicate that SVM based on the NTF method proposed in this study can provide neutron/gamma PSD ability with very high resolution. Presently, this method can become one of the most effective methods for neutron measurement systems, using the digital signal processing technique, as well as the stilbene crystal organic detector.

The promising results obtained encouraged us to validate our proposed process experimentally with other organic scintillator detectors (i.e., plastic and liquid) and time-of-flight methods, as well as testing it in low activity or random detection. We also aim to introduce other artificial intelligence methods to improve the performance of the entire processing method. Furthermore, our NMF/NTF combined with SVM approaches is implemented on DSP and FPGA-based cards to perform real-time tests.

**Author contributions** All authors contributed to the study conception and design. Material preparation, data collection, and analysis were performed by HA. The first draft of the manuscript was written by HA, and all authors commented on previous versions of the manuscript. All authors read and approved the final manuscript.

## References

1. K.-N. Li, X.-P. Zhang, Q. Gui et al., Characterization of the new scintillator Cs<sub>2</sub>LiYCl<sub>6</sub>:Ce<sup>3+</sup>. *Nucl. Sci. Tech.* **29**, 11 (2018). <https://doi.org/10.1007/s41365-017-0342-4>
2. M.L. Roush, M.A. Wilson, W.F. Hornyak, Pulse shape discrimination. *Nucl. Instrum. Methods A* **31**, 112–124 (1964). [https://doi.org/10.1016/0029-554X\(64\)90333-7](https://doi.org/10.1016/0029-554X(64)90333-7)
3. J. Heltsley, L. Brandon, A. Galonsky et al., Particle identification via pulse-shape discrimination with a charge-integrating ADC. *Nucl. Instrum. Methods A* **263**, 441–445 (1988). [https://doi.org/10.1016/0168-9002\(88\)90984-9](https://doi.org/10.1016/0168-9002(88)90984-9)
4. K. Zhou, J. Zhou, Y. Song et al., Compact lithium-glass neutron beam monitor for SANS at CSNS. *Nucl. Sci. Tech* **29**, 127 (2018). <https://doi.org/10.1007/s41365-018-0468-z>
5. E. Bayat, N. Divani-Vais, M.M. Firoozadi et al., A comparative study on neutron-gamma discrimination with NE213 and UGLLT scintillators using zero-crossing method. *Radiat. Phys. Chem.* **81**, 217–220 (2012). <https://doi.org/10.1016/j.radphyschem.2011.10.016>
6. T. He, P. Zheng, J. Xiao, Measurement of the prompt neutron spectrum from thermal-neutron-induced fission in U-235 using the recoil proton method. *Nucl. Sci. Tech* **30**, 112 (2019). <https://doi.org/10.1007/s41365-019-0633-z>
7. M.D. Aspinall, B.D. Mellow, R.O. Mackin et al., Verification of the digital discrimination of neutrons and  $\gamma$  rays using pulse gradient analysis by digital measurement of time of flight. *Nucl. Instrum. Methods A* **583**, 432–438 (2007). <https://doi.org/10.1016/j.nima.2007.09.041>
8. S. Yousefi, L. Lucchese, Digital discrimination of neutrons and gamma-rays in liquid scintillators using wavelets. *Nucl. Instrum. Methods A* **598**, 551–555 (2009). <https://doi.org/10.1016/j.nima.2008.09.028>
9. J.-L. Cai, D.-W. Li, P.-L. Wang et al., Fast pulse sampling module for real-time neutron–gamma discrimination. *Nucl. Sci. Tech* **30**, 84 (2019). <https://doi.org/10.1007/s41365-019-0595-1>
10. P. Raj, A. Raman, *Handbook of Research on Cloud and Fog Computing Infrastructures for Data Science*, 1st edn. (IGI global, Pennsylvania, 2018), pp. 1–400
11. T. Sanderson, C. Scott, M. Flaska et al., Machine learning for digital pulse shape discrimination, in *IEEE Nuclear Science Symposium and Medical Imaging Conference Record*, pp. 1–4 (2012). <https://doi.org/10.1109/NSSMIC.2012.6551092>

12. X. Yu, J. Zhu, S. Lin et al., Neutron/gamma discrimination based on the support vector machine method. *Nucl. Instrum. Methods A* **777**, 80–84 (2015). <https://doi.org/10.1016/j.nima.2014.12.087>
13. W. Zhang, T. Wu, B. Zheng et al., A real-time neutron-gamma discriminator based on the support vector machine method for the time-of-flight neutron spectrometer. *Plasma. Sci. Technol* **20**, 1–6 (2018). <https://doi.org/10.1088/2058-6272/aaaaa9>
14. Z.H. Zhang, C.Y. Hu, X.Y. Fan et al., A direct method of nuclear pulse shape discrimination based on principal component analysis and support vector machine. *J. Instrum.* **14**, 1–10 (2019). <https://doi.org/10.1088/1748-0221/14/06/P06020>
15. P. Krömer, Z. Matej, P. Musílek et al., Neutron-Gamma Classification by Evolutionary Fuzzy Rules and Support Vector Machines, in *IEEE International Conference on Systems, Man, and Cybernetics*, pp. 1–5 (2015). <https://doi.org/10.1109/SMC.2015.461>
16. H. Arahmane, A. Mahmoudi, E.-M. Hamzaoui et al., Neutron-gamma discrimination based on support vector machine combined to nonnegative matrix factorization and continuous wavelet transform. *Measurement* (2020). <https://doi.org/10.1016/j.measurement.2019.106958>
17. A. Cichocki, R. Zdunek, S. Choi et al., Non-negative tensor factorization using alpha and beta divergence, in *IEEE International Conference on Acoustics, Speech and Signal Processing*, pp. 1–4 (2007). <https://doi.org/10.1109/ICASSP.2007.367106>
18. RCA 7265 photomultiplier tube 2" 14-stage s-20, (2014), [http://www.Hofstragroup.Com/product/rca-7265\\_photomultiplier-tube-2-14-stage-s-20/](http://www.Hofstragroup.Com/product/rca-7265_photomultiplier-tube-2-14-stage-s-20/). Accessed 15 July 2014.
19. J.G. Proakis, D.G. Manolakis, *Digital Signal Processing*, 4th edn. (Pearson, London, 2006), p. 1104
20. S. Mallat, *A Wavelet Tour of Signal Processing: The Sparse Way*, 3rd edn. (Academic Press, Cambridge, 2009).
21. A. Muñoz, R. Ertlé, M. Unser, Continuous wavelet transform with arbitrary scales and  $O(N)$  complexity. *Signal Process* **82**, 749–759 (2002). [https://doi.org/10.1016/S0165-1684\(02\)00140-8](https://doi.org/10.1016/S0165-1684(02)00140-8)
22. N. Otsu, A threshold selection method from gray-level histograms. *IEEE. T. Syst. Man. CY-S* **9**, 62–66 (1979). <https://doi.org/10.1109/TSMC.1979.4310076>
23. G. James, D. Witten, T. Hastie, R. Tibshirani, *An Introduction to Statistical Learning with Applications in R* (Springer, New York, 2013).
24. A. Cichocki, R. Zdunek, A.H. Phan et al., *Nonnegative Matrix and Tensor Factorizations: Application to Exploratory Multi-Way Data Analysis and Blind Sources Separation* (Wiley, New Jersey, 2009), p. 500
25. C. Cortes, V. Vapnik, Support-Vector Networks. *Mach. Learn* **20**, 273–297 (1995). <https://doi.org/10.1007/BF00994018>
26. C. Burges, A tutorial on Support Vector Machines for pattern recognition. *Data Min. Knowl. Disc.* **2**(2), 121–167 (1998)
27. J. Mercer, Functions of positive and negative type and their connection with the theory of integral equations. *Philos. Trans. R. Soc. A* **209**, 415–446 (1909). <https://doi.org/10.1098/rsta.1909.0016>
28. G. Valentini, T.G. Dietterich, Bias-variance analysis of support vector machines for the development of SVM-based ensemble methods. *J. Mach. Learn. Res.* **5**, 725–745 (2004). [https://doi.org/10.1007/3-540-45428-4\\_22](https://doi.org/10.1007/3-540-45428-4_22)
29. G. I. Webb, P. Conilione, Estimating bias and variance from data. (CiteSeerX, 2005), <http://citeseerx.ist.psu.edu/viewdoc/summary?doi=10.1.1.71.8679>.
30. H. Arahmane, E.-M. Hamzaoui, R.C. El Moursli, Neutron flux monitoring based on blind source separation algorithms in Moroccan TRIGA MARK II reactor. *Sci. Technol. Nucl. Inst.* **2017**, 1–8 (2017). <https://doi.org/10.1155/2017/5369614>
31. A. Cichocki, S. Amari, *Adaptive Blind Signal and Image Processing: Learning Algorithms and Applications* (Wiley, New Jersey, 2002), p. 586
32. V.V. Vesselinov, M.K. Mudunuru, S. Karra et al., Unsupervised machine learning based on non-negative tensor factorization for analyzing reactive-mixing. *J. Comput. Phys.* **395**, 85–104 (2019). <https://doi.org/10.1016/j.jcp.2019.05.039>
33. H. Arahmane, E.-M. Hamzaoui, Y. Ben Maissa et al., Improving neutron-gamma discrimination with stilbene organic scintillation detector using blind nonnegative matrix and tensor factorization methods. *J. spectrosc.* **2019**, 1–9 (2019). <https://doi.org/10.1155/2019/8360395>
34. H. Arahmane, E.-M. Hamzaoui, R. Cherkaoui El Moursli, Spectrogram analysis of fission chamber's outputs signals using nonnegative matrix and tensor factorization algorithms, in *IEEE International Multi-Conference on Systems, Signals & Devices*, pp. 1–6 (2018). <https://doi.org/10.1109/SSD.2018.8570624>
35. H. Arahmane, E.-M. Hamzaoui, A. Mahmoudi et al., Time-scale characterization of neutron and gamma signals using continuous wavelet transform, in *IEEE International Symposium on signal, Image, Video and Communications*, pp. 1–6 (2018). <https://doi.org/10.1109/ISIVC.2018.8709206>
36. A. Cichocki and R. Zdunek, NMFLAB for signal processing NMFLAB toolboxes. (2006), <http://www.bsp.brain.riken.jp/ICALAB/nmflab>. Accessed 15 June 2006.
37. A.V. Kramarenko, U. Tan, *Int. J. Neurosci.* **113**, 1007–1019 (2002). <https://doi.org/10.1080/00207450390220330>
38. A. Cichocki, R. Zdunek, S. Choi et al., Novel multi-layer non-negative tensor factorization with sparsity constraints, in *Adaptive and Natural Computing Algorithms*, 8th International Conference, ICANNGA 2007, pp. 271–280 (2007). [https://doi.org/10.1007/978-3-540-71629-7\\_31](https://doi.org/10.1007/978-3-540-71629-7_31)